Published in final edited form as:

*Mol Cell Neurosci*. 2016 October ; 76: 33–41. doi:10.1016/j.mcn.2016.08.007.

# Presynaptic CamKII regulates activity-dependent axon terminal growth

**Katherine R. Nesler**[a,1], **Emily L. Starke**[a,1], **Nathan G. Boin**[a], **Matthew Ritz**[a], and **Scott A. Barbee**[a,b,*]

[a]Department of Biological Sciences and Eleanor Roosevelt Institute, University of Denver, Denver, Colorado, 80210 USA

[b]Molecular and Cellular Biophysics Program, University of Denver, Denver, Colorado 80210 USA

## Abstract

Spaced synaptic depolarization induces rapid axon terminal growth and the formation of new synaptic boutons at the *Drosophila* larval neuromuscular junction (NMJ). Here, we identify a novel presynaptic function for the Calcium/Calmodulin-dependent Kinase II (CamKII) protein in the control of activity-dependent synaptic growth. Consistent with this function, we find that both total and phosphorylated CamKII (p-CamKII) are enriched in axon terminals. Interestingly, p-CamKII appears to be enriched at the presynaptic axon terminal membrane. Moreover, levels of total CamKII protein within presynaptic boutons globally increase within one hour following stimulation. These effects correlate with the activity-dependent formation of new presynaptic boutons. The increase in presynaptic CamKII levels is inhibited by treatment with cyclohexamide suggesting a protein-synthesis dependent mechanism. We have previously found that acute spaced stimulation rapidly downregulates levels of neuronal microRNAs (miRNAs) that are required for the control of activity-dependent axon terminal growth at this synapse. The rapid activity-dependent accumulation of CamKII protein within axon terminals is inhibited by overexpression of activity-regulated miR-289 in motor neurons. Experiments *in vitro* using a *CamKII* translational reporter show that miR-289 can directly repress the translation of CamKII via a sequence motif found within the *CamKII* 3’ untranslated region (UTR). Collectively, our studies support the idea that presynaptic CamKII acts downstream of synaptic stimulation and the miRNA pathway to control rapid activity-dependent changes in synapse structure.

### Keywords

CamKII; activity-dependent axon terminal growth; NMJ; miRNA pathway

*Corresponding Author: scott.barbee@du.edu.

[1]These authors contributed equally to this work



**AUTHOR CONTRIBUTIONS:**

Conceived and designed experiments: KRN ELS SAB. Performed the experiments: KRN ELS NGB MR SAB. Analyzed the data: KRN ELS NGB MR SAB. Contributed reagents, materials, and/or analysis tools: KRN ELS NGB MR SAB. Wrote the manuscript: ELS SAB.

## INTRODUCTION

The processes of synaptogenesis and long-term synaptic plasticity involve extensive structural remodeling on both the pre- and postsynaptic side of the synapse. This remodeling is essential for the proper development and function of the nervous system. The axon growth cone is highly dynamic and responds to signals in the surrounding environment directing it to grow towards a target region and ultimately form a synapse on a specific target cell. Importantly, these synapses continue to remodel throughout development and during activity-dependent plasticity. Mechanistically, changes in axon terminals can occur very rapidly (on the order of minutes) and at sites that can be extremely distant (100s to 1000s of microns) from the cell body. To facilitate these rapid changes, local machinery needs to already be in place within the growth cone and presynaptic boutons. Proteins localized to axon terminals include highly conserved components of signal transduction pathways. These mechanisms have been extensively characterized. It has also been shown that specific mRNAs are packaged into transport ribonucleoprotein particles (RNPs) and actively transported into distal axons. These mRNAs are released from repression and subsequently translated in the axonal compartment in response to a local stimulus (Gumy et al., 2014). Local translation provides a mechanism by which axons can rapidly alter their protein composition without requiring direct communication with the nucleus (Jung et al., 2012).

One of the most important secondary messengers in axon growth and guidance is calcium (Sutherland et al., 2014). Increased intracellular $Ca^{2+}$ levels binds to calmodulin (CaM) resulting in the activation of $Ca^{2+}$/CaM-dependent enzymes including calcineurin (CaN), protein kinase A (PKA), and the Calcium/Calmodulin-dependent Kinase II (CamKII) (Faas et al., 2011). In the growth cone, activation of CamKII and PKA promotes attraction and dual inhibition switches this attraction to repulsion (Wen et al., 2004). In presynaptic nerve terminals, a major target for phosphorylation by CamKII is synapsin. The reversible association of synapsin with synaptic vesicles helps to facilitate vesicle clustering and presynaptic plasticity and is controlled by phosphorylation at CamKII and PKA phophorylation sites (Hosaka et al., 1999; Stefani et al., 1997). Recent studies from the Littleton lab (Vasin et al., 2014) have identified a PKA/synapsin-dependent mechanism that is required at the larval *Drosophila* neuromuscular junction (NMJ) to regulate the rapid budding and outgrowth of new presynaptic boutons in response to acute spaced depolarization. While several other signaling mechanisms have been implicated in this process (Ataman et al., 2008; Koon et al., 2011; Korkut et al., 2009; Korkut et al., 2013) little is known about the role of presynaptic CamKII. Furthermore, even less is known about the upstream mechanisms that are involved in the control of activity-dependent presynaptic bouton outgrowth and, more specifically, precisely how these upstream mechanisms are linked to local presynaptic signaling events (Freeman et al., 2011; Nesler et al., 2013; Pradhan et al., 2012).

In mammals and flies, CamKII expression can be post-transcriptionally regulated at the level of translation. The activity-dependant translation of the *CamKII* mRNA in *Drosophila* olfactory projection neuron (PN) dendrites requires components of the microRNA (miRNA)-containing RNA induced silencing complex (RISC) (Ashraf et al., 2006). Similar results

have been observed in mammalian hippocampal neurons (Banerjee et al., 2009). In both cases, this is facilitated via the rapid activity-dependent degradation of the SDE3 helicase Armitage (MOV10 in mammals). Degradation of Armitage/MOV10, and potentially other RISC components, is thought to destabilize the apparatus required for miRNA-mediated mRNA regulation (Ashraf et al., 2006; Banerjee et al., 2009). Consistent with this hypothesis, rapid degradation of miRNAs occurs in mammalian neurons in response to activity (Krol et al., 2010).

Similarly, we have shown that spaced stimulation rapidly downregulates levels of five miRNAs in *Drosophila* larval ventral ganglia (Nesler et al., 2013). We demonstrated that three of these miRNAs (miRs-8, -289, and -958) control rapid presynaptic bouton growth at the larval NMJ. We focus here on CamKII because the fly *CamKII* 3' untranslated region (UTR) contains two putative binding sites for activity-regulated miR-289 (Ashraf et al., 2006). This suggests that 1) the CamKII protein might be required to control activity-dependent axon terminal growth, and 2) the *CamKII* mRNA may be a downstream target for regulation by neuronal miR-289.

In this study, we show that knockdown of *CamKII* within the presynaptic compartment using transgenic RNAi disrupts activity-dependent presynaptic growth. We demonstrate that phosphorylated CamKII (p-CamKII) is enriched at the presynaptic axon terminal membrane. We also find that spaced stimulation rapidly leads to a global increase in total CamKII protein levels within axon terminals. This increase can be blocked by treatment with either the translational inhibitor cyclohexamide or presynaptic overexpression of miR-289. Together, this suggests a translation-dependent mechanism. Using an *in vitro* translational reporter fused to the *CamKII* 3'UTR, we show that *CamKII* expression is downregulated by miR-289 via one binding site. Collectively, these data provide support for the idea that CamKII is acting downstream of activity-regulated miRNAs to control rapid activity-dependent presynaptic plasticity.

## MATERIALS AND METHODS

### Fly strains

All *Drosophila* stocks were cultured at 25°C on standard Bloomington medium. Stocks were obtained from the following sources: *Canton-S, $w^{1118}$ (Iso31), UAS-CamKII$^{Ala}$, UAS-CamKII$^{R3(WT)}$, UAS-CamKII$^{T287A}$, UAS-CamKII$^{T287D}$*, and *C380-Gal4* (Bloomington *Drosophila* Stock Center); *UAS-CamKII$^{v38930}$* and *UAS-CamKII$^{v47280}$* long hairpin RNAi lines (Vienna *Drosophila* Resource Center) (Dietzl et al., 2007); *UAS-CamKII:EYFP-CamKII 3'UTR* and *UAS-CamKII:EYFP-NUT 3'UTR* were gifts from S. Kunes (Ashraf et al., 2006); *UAS-mCherry: miR-289 pri-miRNA* was from Barbee lab stocks (Nesler et al., 2013).

### Activity paradigm

The acute spaced synaptic depolarization assay was done exactly as we have previously described (Nesler et al., 2013). Where indicated, cyclohexamide (100 mM) was added to normal HL3 haemolymph-like dissection buffer during the entire rest phase. Following the

rest phase, larvae were checked to make sure that they were alive and then processed for NMJ analysis.

## Immunohistochemistry

NMJ dissection, immunostaining, and the quantification of boutons were done as we have previously described (Nesler et al., 2013; Pradhan et al., 2012). We used the following primary antibodies: mouse anti-CamKII 1:2000 (Takamatsu et al., 2003) (Cosmo), rabbit anti-CamKII 1:4000 (Koh et al., 1999), anti-DLG 1:100 (4F3; deposited to the Developmental Studies Hybridoma Bank by C. Goodman), anti-DVGLUT 1:10,000 (Daniels et al., 2004), anti-pT287 CamKII 1:150 (Santa Cruz), and anti-GFP 1:2500 (TP401; Torrey Pines). Secondary antibodies conjugated to Alexa Fluor® 488, 568, and 633 (Molecular Probes) were used at a concentration of 1:500. Antibodies against HRP conjugated to Dylight™ 594 and 647 (Jackson Labs) were used at 1:500 and added with secondary antibodies. All images were acquired on an Olympus FV1000 scanning confocal microscope using either a 60X (N.A. 1.42) or 100X objective (N.A. = 1.4). Unless otherwise indicated, images presented have been combined using FV1000 software from confocal stacks collected at intervals of 0.4 μM.

## Quantitative immunofluorescence and western analysis

For quantitative confocal microscopy of CamKII immunofluorescence, larvae from 0X and 5X high $K^+$ treatment groups were dissected on the same day and then processed for immunochemistry in the same dish to ensure that antibody staining was consistent. All images were acquired using identical settings on the scanning confocal microscope. Initial settings were established for each paired experiment by thresholding the red and green channels to the brightest NMJs identified in the 5X high $K^+$ treatment group. Following imaging, the intensity of CamKII fluorescence relative to either HRP or DvGLUT was analyzed using two distinct methods to identify regions of interest (ROIs) using ImageJ v1.45 open source software (NIH). The initial steps in both processes were identical. First, RGB images were split into their corresponding channels and then uniformly zoomed to 150% for analysis. Next, the ROI manager was opened to compile a list of ROIs as defined by either boutons demarked by HRP or DvGLUT positive puncta. For HRP images specifically, ROIs were selected in the HRP channel (red) by using the “freehand selections tool” carefully tracing around each individual bouton and adding them to the ROI list. Alternatively, for DvGLUT puncta, the ROIs were selected using a thresholding approach. First, the image in the DvGLUT channel (red) was auto-thresholded. Next, the DvGLUT puncta were selected and added to the ROI manager for measurement. Then the image was closed and re-opened, colors split again, keeping all of the data points in the ROI manager. This was done so that the red channel was no longer thresholded due to the fact that thresholding the image eliminates the variability in puncta intensity. In both cases, ROIs were superimposed on the CamKII channel (green). Measurements were taken for both the green and red channels using the “mean gray value” in ImageJ. Following quantification for the entire data set, a mean value for green intensity (CamKII) and red intensity (HRP or DvGLUT, depending on the experiment) was calculated for each NMJ. This was done so that the data was not biased in favor or those NMJs containing a greater number of ROIs.

Finally, a ratio was calculated (green/red) for each NMJ and recorded. This data was then exported for statistical analysis.

For quantitative western blotting, the CNS (ventral ganglion plus optic lobes minus eye imaginal discs) was dissected from 15 larvae from 0X and 5X high $K^+$ treatment groups (each). This CNS tissue was homogenized directly in 2X Laemmli sample buffer (BioRad), clarified by centrifugation, and the entire supernatant separated by SDS-PAGE. The following primary antibodies were used: anti-CamKII 1:4000 (Cosmo) and anti-actin 1:1000 (Cell Signaling). Secondary antibodies conjugated to HRP (Cell Signaling Technology) were used at a dilution of 1:1000. Band intensities from scanned images were determined using ImageJ (NIH).

### Cell culture

*Drosophila* Schneider 2 (S2-DRSC isolate) cells were cultured and transfected with expression plasmids essentially as we have previously described (Nesler et al., 2013) except that all transfections were performed in three biological replicates in 12-well plates using Effectene transfection reagent (Qiagen). The transfection mixtures for each well contained 50 ng of the firefly luciferase (FLuc) *CamKII* 3'UTR reporter, 200 ng of a *Renilla* luciferase transfection control, and 250 ng of either a pre-miR expression vector or an empty vector control. Most vectors are described elsewhere (Nesler et al., 2013). The wild-type *CamKII* 3'UTR was cloned into pENTR (Invitrogen) using the following primers: CKIIf 5'-CCCATCAGTCCGAGGAG ACG-3' and CKIIr 5'-TGTTTGTGCATTAGCGTCCCA-3' and then into a pAc5.1-FLuc2 [dPolyA] destination vector. Mutations were introduced at nucleotides 727–729 within the seed region interacting sequence in miR-289 binding site 2 (QuikChange SDM Kit; Strategene).

### Statistics

All statistical analysis including graphing was done using Prism software (GraphPad) and statistical significance determined to be at $p < 0.05$. In all bar graphs, the mean is presented ± SEM. When two samples are compared, we used a paired Student's t-test. When more than two samples are compared, we used a one-way ANOVA with a Tukey's post-hoc test. In experiments where ghost bouton quantification was required, statistical outliers were eliminated using the ROUT method (robust regression and outlier removal; Q = 1%) (Motulsky and Brown, 2006).

## RESULTS and DISCUSSION

### Presynaptic CamKII is necessary for activity-dependent axon terminal growth

Acute spaced synaptic depolarization rapidly induces the formation of new synaptic boutons at the larval NMJ (Ataman et al., 2008; Vasin et al., 2014). These immature presynaptic outgrowths, also known as "ghost boutons", are characterized by the presence of synaptic vesicles but by a lack of active zones and postsynaptic specializations (Ataman et al., 2006). In our hands, a wild-type third instar larval NMJ will typically have about 2 ghost boutons (Fig. 1B, D; 0X high $K^+$, 1.7 ± 0.2 ghost boutons per NMJ). Using an established synaptic growth protocol, we observed a robust increase in the number of ghost boutons following 5X

$K^+$ spaced stimulation (Fig. 1A; stimulation protocol was adapted from Ataman et al., 2008; Fig. 1B, D; 3.3-fold increase relative to unstimulated controls; 5X high $K^+$, 5.6 ± 1.0; $p < 0.0001$). It has been shown that activity-dependent ghost bouton formation involves both new gene transcription and protein synthesis (Ataman et al., 2008). Furthermore, new presynaptic expansions can form within 30 minutes of stimulation even after the axon innervating the NMJ has been severed (Vasin et al., 2014). These findings suggest that a local mechanism (i.e. local signaling and/or translation) is required for the budding and outgrowth of new axon terminals. As expected, application of the translational inhibitor cyclohexamide during the recovery phase prevented the formation of new ghost boutons (Fig. 1D; 0X high $K^+$, 2.3 ± 0.4; 5X high $K^+$, 2.6 ± 0.4).

We have shown previously that the outgrowth of new synaptic boutons in response to spaced depolarization requires the function of activity-regulated neuronal miRNAs including miR-8, miR-289, and miR-958 (Nesler et al., 2013). This implies that mRNAs encoding for synaptic proteins might be targets for regulation by these miRNAs. We focused on CamKII for three reasons. 1) CamKII has been shown to have a conserved role in the control of long-term synaptic plasticity and its expression at synapses requires components of the miRNA pathway (Ashraf et al., 2006). Furthermore, the fly *CamKII* mRNA contains two predicted binding sites for activity-regulated miR-289. 2) CamKII and PKA both phosphorylate and actives synapsin (Hosaka et al., 1999; Stefani et al., 1997). At the fly NMJ, a synapsin-dependent mechanism is required for a transient increase in neurotransmitter release in response to tetanic stimulation (Akbergenova and Bykhovskaia, 2007; Kuromi and Kidokoro, 2002). Synapsin also redistributes to sites of activity-dependent axon terminal growth and regulates outgrowth via a PKA-dependent pathway (Vasin et al., 2014). 3) Presynaptic CamKII has been shown to function in axon pathfinding in cultured *Xenopus* neurons (Wen et al., 2004). It seemed likely that activity-dependent ghost bouton formation and axon guidance might share similar molecular machinery.

We postulated that presynaptic CamKII was required to control activity-dependent axon terminal growth at the larval NMJ. To address this question, we first disrupted CamKII expression in motor neurons using two transgenic RNAi constructs. Depletion of presynaptic CamKII with both transgenes prevented the formation of new ghost boutons in response to spaced stimulation (Fig. 1C, D; *C380-Gal4>UAS-CamKII*$^{v38930}$ 0X high $K^+$, 0.8 ± 0.2 and 5X high $K^+$, 0.7 ± 0.2; *C380-Gal4>UAS-CamKII*$^{v47280}$ 0X high $K^+$, 1.1 ± 0.3 and 5X high $K^+$, 1.7 ± 0.3). Thus, presynaptic CamKII is necessary to control the formation of new synaptic boutons.

To further confirm that presynaptic CamKII function was required for activity-dependent growth, we used a transgenic line that inducibly expressed an inhibitory peptide (*UAS-CamKII*$^{Ala}$). As in mammals, the activation of *Drosophila* CamKII by exposure to calcium leads to the autophosphorylation of a conserved threonine residue within the autoinhibitory domain (T287 in *Drosophila*). Activation of CamKII then confers an independence to calcium levels that persists until threonine-287 is dephosphorylated (Wang et al., 1998). The synthetic Ala peptide mimics the autoinhibitory domain and its transgenic expression is sufficient to substantially inhibit endogenous CamKII activity (Joiner and Griffith, 1997). Expression of the Ala inhibitory peptide in larval motor neurons disrupted the formation of

new ghost boutons following spaced synaptic depolarization (Fig. 1D; *C380-Gal4>UAS-CamKII$^{Ala}$* 0X high $K^+$, 1.7 ± 0.3 and 5X high $K^+$, 2.6 ± 0.3). These observations are consistent with results from CamKII RNAi.

Together, our data suggest that presynaptic CamKII function is required to control new ghost bouton formation in response to acute synaptic activity. Similarly, presynaptic CamKII has been implicated in controlling both bouton number and morphology during development of the larval NMJ. Reducing neuronal CamKII levels by RNAi has recently been shown to significantly reduce the number of type 1b boutons at the larval NMJ suggesting that presynaptic CamKII is required to control normal synapse development (Gillespie and Hodge, 2013). In contrast, presynaptic expression of the Ala inhibitory peptide has no effect on the total number of type 1 synaptic boutons (Haghighi et al., 2003; Koh et al., 1999; Morimoto et al., 2010). Given that the Ala peptide does not completely inhibit CamKII autophosphorylation, we suggest that the activation of CamKII in response to acute spaced synaptic depolarization is likely to be more sensitive to disruption then during NMJ development (Griffith et al., 1993; Jin et al., 1998).

## Presynaptic overexpression of CamKII does not enhance activity-dependent growth

We next asked if presynaptic CamKII could induce activity-dependent axon terminal growth at the NMJ. The overexpression of genes that are necessary for the control of ghost bouton formation generally does not cause an increase in the overall number of new synaptic boutons following 5X high $K^+$ spaced stimulation (Ataman et al., 2008; Nesler et al., 2013; Vasin et al., 2014). Instead, overexpression often leads to an increased sensitization of the synapse to subsequent stimuli (for example, significant growth is observed after 3X instead of 5X high $K^+$). The overexpression of a wild-type CamKII transgene in motor neurons caused an increase of 71% in ghost bouton numbers in 3X $K^+$ spaced stimulation larvae compared to 0X $K^+$ controls (Fig. 1E; *C380-Gal4>UAS-CamKII$^{WT}$*; 0X high $K^+$, 2.7 ± 0.4; 3X high $K^+$, 4.6 ± 0.7; p = 0.11). While this is trending towards an increase, it did not reach statistical significance, even though expression levels were substantially higher than endogenous CamKII (Fig. S1). Thus, increased CamKII is not sufficient to stimulate activity-dependent axon terminal growth.

To further investigate the role of presynaptic CamKII in activity-dependent axon terminal growth, we examined the effect of transgenic neuronal overexpression of either an overactive form of CamKII (CamKII$^{T287D}$) or a form that is incapable of remaining active in the absence of elevated calcium (CamKII$^{T287A}$). Much like *C380-Gal4/+* controls, presynaptic expression of either transgene had no significant effect on the number of ghost boutons in 3X high $K^+$ stimulation larvae (Fig. 1E; *C380-Gal4>UAS-CamKII$^{T287D}$*, 18% increase, 0X high $K^+$, 3.3 ± 0.6; 3X high $K^+$, 3.9 ± 0.5, p = 0.88; *C380-Gal4>UAS-CamKII$^{T287A}$*, 45% decrease, 0X high $K^+$, 3.3 ± 0.6; 3X high $K^+$, 1.8 ± 0.3, p = 0.37). Again, levels of CamKII protein in axon terminals in both transgenic lines were elevated relative to controls (Fig. S1). Collectively, these data suggest that constitutive activation of CamKII is not sufficient to sensitize the NMJ to stimulation.

Our results suggest that the temporal and/or spatial regulation of CamKII expression or activation is likely required to control activity-dependent growth. In support, the *Drosophila*

CamKII protein has been shown to phosphorylate and regulate the activity of the Ether-a-go-go (Eag) potassium channel in motor neuron axon terminals (Wang et al., 2002). In turn, CamKII is bound and locally activated by phosphorylated Eag (Sun et al., 2004). This local activation can persist even after calcium levels have been reduced. CamKII autophosphorylation and Eag localization to synapses requires the activity of the membrane-associated Calcium/Calmodulin-associated Serine Kinase, CASK (Gillespie and Hodge, 2013). The presynaptic coexpression of CASK with CamKII$^{T287D}$ reverses (to wild-type levels) the increase in type 1b boutons observed when CamKII$^{T287D}$ is overexpressed alone. Thus, a mechanism exists at the larval NMJ that allows for the persistence of local CamKII activation in the absence of additional stimuli.

## CamKII is primarily enriched in axon terminals at the Drosophila larval NMJ

After establishing that CamKII has a novel presynaptic function in activity-dependent ghost bouton formation, we next sought to closely examine the distribution of CamKII protein at the larval NMJ. It has previously been reported that CamKII strongly colocalizes with postsynaptic Discs large (DLG), the *Drosophila* ortholog of mammalian PSD-95, around the borders of type 1 synaptic boutons. In support, an anti-CamKII antibody coimmunoprecipitates DLG from larval body wall extracts (Koh et al., 1999). Interestingly, while DLG is pre-dominantly postsynaptic at the developing NMJ it is also initially expressed in the presynaptic cell and at least partially overlaps with presynaptic membrane markers in axon terminals (Guan et al., 1996; Lahey et al., 1994). The studies of Ashraf et al. (2006) have demonstrated that while fly CamKII colocalizes with DLG within dendrites of adult olfactory projection neurons (PNs), it also localizes to presynaptic boutons within those same neurons. Consistent with the latter observations (using a different CamKII antibody), it has been shown that CamKII is substantially enriched in presynaptic terminals of type 1b boutons (Gillespie and Hodge, 2013; Takamatsu et al., 2003). To resolve these inconsistent results, we have used both antibodies against CamKII to more closely analyze the localization of CamKII at the third instar larval NMJ. First, double labeling of wild-type NMJs with a monoclonal CamKII antibody and anti-horseradish peroxidase (HRP), a marker for *Drosophila* neurons, confirmed that CamKII was enriched in presynaptic boutons in a pattern very similar to that of HRP (Fig. 2A) (Takamatsu et al., 2003). A closer examination of confocal optical sections revealed that almost all CamKII localized to the presynaptic terminal and was not significantly enriched either 1) at sites surrounding presynaptic boutons (Fig. 2A’), or 2) in the axons innervating synaptic arbors (Fig. 2A; arrowhead).

Within boutons, CamKII appeared to be predominantly cytoplasmic but was sometimes localized to discrete puncta that were reminiscent of antibody staining for active zones. Prolonged depolarization of hippocampal neurons with $K^+$ leads to mobilization of CamKII from the cytoplasm to sites near active zones (Tao-Cheng et al., 2006). Moreover, using a fluorescent reporter for CamKII activity, high frequency stimulation causes the very rapid (on the order of minutes) activation of presynaptic CamKII and promotes its translocation from the cytoplasm to sites near active zones (Shakiryanova et al., 2011). To address this possibility, we double labeled larval NMJs with antibodies targeting both CamKII (Takamatsu et al., 2003) and DVGLUT, the *Drosophila* vesicular glutamate transporter, in

order to visualize active zones (Daniels et al., 2004). As predicted, we found that some presynaptic CamKII colocalized with DVGLUT in type 1b and 1s boutons (Fig. 2B; 1b bouton indicated by arrow; 1s bouton indicated by arrowhead). Thus, in some type 1 synaptic boutons, CamKII protein is enriched in or near active zones.

To demonstrate the specificity of the CamKII monoclonal antibody, we next disrupted the expression of neuronal CamKII using our two transgenic CamKII-targeting RNAi constructs (both used in Fig. 1). Presynaptic *CamKII* RNAi completely disrupted expression of CamKII in axon terminals (Fig. 2C). A faint halo of CamKII remained around the border of synaptic boutons following RNAi (Fig. 2C; arrowhead). This residual immunostaining likely represents the population of CamKII expressed in muscle and localized at or near postsynaptic densities. To further confirm that CamKII was enriched in presynaptic boutons, we double labeled wild-type NMJs with a polyclonal CamKII antibody and anti-DLG (Koh et al., 1999). As previously shown, CamKII did partially colocalize with DLG at the border of type 1 synaptic boutons (Fig. 2D). However, in our hands, CamKII was primarily localized to the presynaptic side of the synapse. Collectively, we provide strong evidence that CamKII is expressed on both the pre- and postsynaptic side of the synapse but that it is clearly enriched within presynaptic boutons at the larval NMJ. This localization is analogous to CamKII distribution in mammalian axons.

## Motoneuron axon terminals are enriched for phosphorylated CamKII

After demonstrating that total CamKII was enriched in presynaptic axon terminals, we next asked if any of this protein was active by assessing phosphorylation of threonine-287 using a phospho-specific polyclonal antibody (Gillespie and Hodge, 2013). We found that pT287 CamKII staining intensity was strong and fairly uniform in presynaptic boutons (Fig. 3A; arrow) and weakly stained axons innervating synaptic arbors (Fig. 3A; arrowhead). Closer examination of confocal optical sections revealed that almost all p-CamKII colocalized with HRP in the presynaptic terminal and only sparsely stained the body wall muscle (Fig. 3A’). Presynaptic *CamKII* RNAi almost completely disrupted p-CamKII in axon terminals leaving some residual staining in the presynaptic bouton and surrounding muscle suggesting that the antibody is specific (Fig. 3B). To further demonstrate this presynaptic localization, we found that p-CamKII staining clearly does not overlap with postsynaptic DLG (Fig. 3C) but does colocalize strongly with immunostaining using the monoclonal total CamKII antibody (Fig. 3D).

## Enrichment of CamKII in motoneuron axon terminals does not require the CamKII 3’UTR

Collectively, we have used three different antibodies to show that CamKII enriched in presynaptic axon terminals. Next, we were curious as to how this enrichment was occurring. In *Drosophila* and mammalian neurons, the *CamKII* mRNA is transported to dendritic compartments and locally translated in response to synaptic stimulation (Aakalu et al., 2001; Ashraf et al., 2006). This spatial and temporal regulation requires sequence motifs found within the 5’ and 3’ UTRs of the *CamKII* transcript. In contrast, the localization of CamKII to axon terminals of *Drosophila* PNs does not strictly require the *CamKII* 3’UTR suggesting that enrichment in presynaptic boutons occurs through a mechanism that does not strictly require local translation (Ashraf et al., 2006). In mammalian neurons, CamKII is enriched in

axon terminals where it can associate with synaptic vesicles and synapsin I (Benfenati et al., 1996; Benfenati et al., 1992). Recently, it has been shown that mammalian CamKII and the synapsin proteins are both conveyed to distal axons at rates consistent with slow axonal transport, with a small fraction of synapsin cotransported with vesicles via fast transport (Scott et al., 2011).

Because activity-dependent growth at the larval NMJ requires the miRNA pathway and new protein synthesis (Fig. 1D) (Ataman et al., 2008; Nesler et al., 2013), we asked if the localization of CamKII protein to axon terminals might require the *CamKII* 3'UTR. As expected, when expression was specifically driven in larval motor neurons, a transgenic CamKII:EYFP fusion protein regulated by the *CamKII* 3'UTR localized strongly to presynaptic boutons at the larval NMJ (Fig. 4A; *C380-Gal4>UAS-CamKII:EYFP:CamKII 3'UTR*). However, very similar results were observed using the same CamKII:EYFP fusion protein regulated by a heterologous 3'UTR (Fig. 4B; *C380-Gal4>UAS-CamKII:EYFP:NUT 3'UTR*). Taken together, these data suggest that localization of CamKII protein to presynaptic boutons at the NMJ does not require mRNA transport and local translation. Thus, we conclude that most of the *Drosophila* CamKII protein found in motoneuron axon terminals is likely there due to the transport of cytosolic CamKII from the cell body to synapses via a mechanism involving axonal transport.

## CamKII levels in axon terminals rapidly increase in response to spaced synaptic stimulation

We were interested in determining how CamKII might be regulating activity-dependent axon terminal growth and speculated that either the levels or distribution of CamKII protein might be altered in response to spaced depolarization. We first asked if high $K^+$ stimulation resulted in an increase in CamKII protein within motoneuron axon terminals. Larval preparations were stimulated as shown in Fig. 1A and changes in the levels of CamKII protein in presynaptic boutons was examined by immunohistochemistry and quantitative confocal microscopy (Fig. 5A–B). Following spaced stimulation, CamKII staining within boutons rapidly increased (in ~1 hour) by an average of 26% (Fig. 5B; $p < 0.05$). This increase in immunofluorescence was global and did not appear to be localized to particular regions of the NMJ (i.e. near obvious presynaptic outgrowths). CamKII has been reported to very rapidly translocate to regions near active zones in response to high frequency stimulation (Shakiryanova et al., 2011). However, when compared to DVGLUT levels in unstimulated and stimulated larvae, no significant increase in CamKII immunoflourescence was observed indicating that translocation does not occur or does not persist in our assay (Fig. 5B). To determine if this increase in CamKII enrichment required new protein synthesis, we incubated larval preparations with the translational inhibitor cyclohexamide during the recovery phase (as in Fig. 1). Surprisingly, this treatment completely blocked the activity-dependent affects on presynaptic CamKII enrichment within axon terminals (Fig. 5B). Thus, spaced high $K^+$ stimulation results in a rapid increase in CamKII levels in presynaptic boutons via some mechanism that requires activity-dependent protein synthesis.

Next, we asked if the levels or distribution of p-CamKII changed in response to spaced stimulation. Larval preparations were stimulated exactly as described above and analyzed by

confocal microscopy (Fig. 5C). Interestingly, p-CamKII staining was enriched at the presynaptic membrane of many axon terminals following spaced depolarization (Fig. 5C; arrows).

Given the requirement for new protein synthesis, we speculated that the additional CamKII protein in axon terminals could be derived from a pool of CamKII *mRNA* that is rapidly transcribed and translated in the soma in response to spaced depolarization. This newly translated CamKII would then be actively transported out to axon terminals via standard mechanisms. If this were true, we would expect to detect elevated CamKII levels in the larval ventral ganglion. To examine this process more closely, global total CamKII expression levels within the larval ventral ganglion were assayed by Western blot analysis. We found that two distinct isoforms of CamKII are expressed in explanted larval ventral ganglia (97 and 116 kDa; Fig. 5D). Surprisingly, we did not observe an increase in CamKII protein levels in the ventral ganglion.

What is the source of this new presynaptic CamKII protein? We propose there are three possible explanations. First, new CamKII protein might be transcribed and translated in the motor neuron cell body. However, this new protein would be rapidly transported away to axon terminals in response to spaced depolarization. Second, some CamKII protein is found in the axons innervating the NMJ (seen using the p-CamKII antibody; Fig. 3A; arrowhead). It is possible that activity stimulates the rapid transport of an existing pool of CamKII protein from distal axons into axon terminals. This process would be sensitive to translational inhibitors. Finally, a pool of *CamKII* mRNA might be actively transported into axon terminals and then locally translated in response to spaced depolarization. This would account for the both the dependence on translation and for increased CamKII enrichment in presynaptic boutons.

### CamKII enrichment in axon terminals is negatively regulated by miR-289

Thus far, we have shown that activity-dependent ghost bouton formation correlates with a protein synthesis-dependent increase in CamKII levels within presynaptic boutons at the larval NMJ. The activity-dependent translation of CamKII in olfactory neuron dendrites in the adult *Drosophila* brain requires components of the miRNA pathway (Ashraf et al., 2006). Within the *CamKII* 3'UTR, there are two putative binding sites for activity-regulated miR-289 (Fig. 6A). These two binding sites were of particular interest. We have previously shown that levels of mature miR-289 are rapidly downregulated in the larval brain in response to 5X high $K^+$ spaced training (Nesler et al., 2013). Moreover, presynaptic overexpression of miR-289 significantly inhibits activity-dependent ghost bouton formation at the larval NMJ (Nesler et al., 2013). Based on these data, we speculated that CamKII might be a target for regulation by miR-289.

To determine if CamKII is a target for repression by miR-289 *in vivo*, we overexpressed a transgenic construct containing the primary miR-289 transcript in motor neurons and examined CamKII enrichment by anti-CamKII immunostaining and quantitative confocal microscopy (Fig. 6B). Relative to controls, the presynaptic overexpression of miR-289 completely abolished the observed activity-dependent increase in CamKII immunofluorescence (*C380-Gal4/+* controls, 20% increase in 5X high $K^+$ group, $p < 0.05$;

*C380-Gal4>UAS-pri-miR289*, 3% increase, $p = 0.73$). When analyzing global CamKII levels within axon terminals during NMJ development, presynaptic miR-289 expression led to a slight decrease in CamKII immunofluorescence (Fig. 6B; *C380-Gal4>UAS-pri-miR289*, 13% decrease in 0X high $K^+$ group, $p = 0.06$). This trend is similar to results observed following treatment with cyclohexamide during the recover period (Fig. 5B). The lack of full repression by miR-289 is not surprising given that one miRNA alone is often not sufficient to completely repress target gene expression (Thomas et al., 2010).

To directly test the ability of miR-289 to repress translation of *CamKII*, we developed a reporter where the coding sequence for firefly luciferase (FLuc) was fused to the regulatory *CamKII* 3'UTR (*FLuc-CamKII 3'UTR*; Fig. 6C). When this wild-type reporter was coexpressed with miR-289 in *Drosophila* S2 cells, expression of FLuc was significantly reduced (Fig. 6D; 30% of empty vector controls, $p < 0.0001$). In contrast, when this reporter was coexpressed with miR-279a, a miRNA not predicted to bind to the *CamKII* 3'UTR, no repression was observed (99% of controls, $p = 0.99$). To confirm that repression of the *FLuc-CamKII* reporter by miR-289 was via a specific interaction, we mutagenized the second of two predicted miR-289 binding sites (Fig.6A and 6C). Binding site 2 (BS2) was a stronger candidate for regulation because it is flanked by AU-rich elements (AREs) and miR-289 has been shown to promote ARE-mediated mRNA instability through these sequences (Jing et al., 2005). Moreover, it is well established that the stabilization and destabilization of neuronal mRNAs via interactions between AREs and ARE-binding factors plays a significant role in the establishment and maintenance of long-term synaptic plasticity in both vertebrates and invertebrates (Lee et al., 2015). Altering three nucleotides within BS2 in the required seed region binding site was sufficient to significantly disrupt repression of the reporter by miR-289 (Fig. 6E; compare the wild-type 3'UTR, 44% of control; and BS2mut, 85% of control, $p < 0.0001$). We also cloned the minimal predicted BS2 sequence into an unrelated 3'UTR and asked if miR-289 could repress translation (Fig. 6C). Coexpression of the FLuc-SV-mBS2 reporter with miR-289 led to significant repression (Fig. 6E; 62% of control; $p < 0.0001$). Taken together, these results indicate that the BS2 sequence is both necessary and sufficient for miR-289 regulation via the *CamKII* 3'UTR.

## CONCLUSION

The most important conclusion of this study is that presynaptic CamKII is required to control activity-dependent axon terminal growth at the *Drosophila* larval NMJ. First, we show that CamKII is necessary to control ghost bouton formation in response to spaced synaptic depolarization (Fig. 1D–E). Next, we demonstrate that spaced stimulation correlates with a rapid protein synthesis dependent increase in CamKII immunofluorescence in presynaptic boutons (Fig. 5A–B). This increase is suppressed by presynaptic overexpression of activity-regulated miR-289 (Fig. 6B). We have previously shown that overexpression of miR-289 in larval motor neurons can suppress activity-dependent axon terminal growth (Nesler et al., 2013). Here, we demonstrate that miR-289 can repress the translation of a *FLuc-CamKII* 3'UTR reporter via a specific interaction with a binding site within the *CamKII* 3'UTR (Fig. 6C–E). Collectively, this experimental evidence suggests that CamKII functions downstream of the miRNA pathway to control activity-dependent changes in synapse structure.

Thus, CamKII protein is expressed in the right place to regulate rapid events that are occurring within presynaptic boutons. Several questions remain regarding CamKII function in the control of activity-dependent axon terminal growth. First, it is unclear what the significance might be of a rapid increase of total CamKII in presynaptic terminals. Why is the pool of CamKII protein that is already present not sufficient to control these processes? Similar questions have been asked regarding activity-dependent processes occurring within dendrites. We postulate that the *CamKII* mRNA might be locally translated in axon terminals. It has been proposed that local mRNA translation might be 1) required for efficient targeting of some synaptic proteins to specific sites, or 2) local translation may in and of itself be required to control activity-dependent processes at the synapse (Steward, 2002). Second, the impact of spaced depolarization on CamKII function needs to be assessed and downstream targets of CamKII phosphorylation involved in these processes need to be identified. One very strong candidate is synapsin which, at the *Drosophila* NMJ, has been shown to rapidly redistribute to sites of new ghost bouton outgrowth in response to spaced stimulation (Vasin et al., 2014). Finally, the idea that CamKII might work through a Eag/CASK-dependent mechanism to control activity-dependent axon terminal growth needs to be explored (Gillespie and Hodge, 2013).

## Supplementary Material

Refer to Web version on PubMed Central for supplementary material.

## Acknowledgments

We would like to thank present and former members of the Barbee lab for assistance with image analysis, critical reading of the manuscript, and useful discussions. The work presented here was supported by a NIH grant to SAB (DA026048). MR was also supported by a DU undergraduate PINS grant. Stocks obtained from the Bloomington *Drosophila* Stock Center (funded by NIH P40OD018537) were used in this study. The anti-DLG monoclonal antibody was obtained from the Developmental Studies Hybridoma Bank, which was created by the NICHD at the NIH and is maintained at the University of Iowa. Both miRBase (www.mirbase.org) and Flybase (www.flybase.org) provided essential information.

## REFERENCES

Aakalu G, Smith WB, Nguyen N, Jiang C, Schuman EM. Dynamic visualization of local protein synthesis in hippocampal neurons. Neuron. 2001; 30:489–502. [PubMed: 11395009]

Akbergenova Y, Bykhovskaia M. Synapsin maintains the reserve vesicle pool and spatial segregation of the recycling pool in Drosophila presynaptic boutons. Brain research. 2007; 1178:52–64. [PubMed: 17904536]

Ashraf SI, McLoon AL, Sclarsic SM, Kunes S. Synaptic protein synthesis associated with memory is regulated by the RISC pathway in Drosophila. Cell. 2006; 124:191–205. [PubMed: 16413491]

Ataman B, Ashley J, Gorczyca D, Gorczyca M, Mathew D, Wichmann C, Sigrist SJ, Budnik V. Nuclear trafficking of Drosophila Frizzled-2 during synapse development requires the PDZ protein dGRIP. Proceedings of the National Academy of Sciences of the United States of America. 2006; 103:7841–7846. [PubMed: 16682643]

Ataman B, Ashley J, Gorczyca M, Ramachandran P, Fouquet W, Sigrist SJ, Budnik V. Rapid activity-dependent modifications in synaptic structure and function require bidirectional Wnt signaling. Neuron. 2008; 57:705–718. [PubMed: 18341991]

Banerjee S, Neveu P, Kosik KS. A coordinated local translational control point at the synapse involving relief from silencing and MOV10 degradation. Neuron. 2009; 64:871–884. [PubMed: 20064393]

Benfenati F, Onofri F, Czernik AJ, Valtorta F. Biochemical and functional characterization of the synaptic vesicle-associated form of CA2+/calmodulin-dependent protein kinase II. Brain Res Mol Brain Res. 1996; 40:297–309. [PubMed: 8872314]

Benfenati F, Valtorta F, Rubenstein JL, Gorelick FS, Greengard P, Czernik AJ. Synaptic vesicle-associated Ca2+/calmodulin-dependent protein kinase II is a binding protein for synapsin I. Nature. 1992; 359:417–420. [PubMed: 1328883]

Daniels RW, Collins CA, Gelfand MV, Dant J, Brooks ES, Krantz DE, DiAntonio A. Increased expression of the Drosophila vesicular glutamate transporter leads to excess glutamate release and a compensatory decrease in quantal content. J Neurosci. 2004; 24:10466–10474. [PubMed: 15548661]

Dietzl G, Chen D, Schnorrer F, Su KC, Barinova Y, Fellner M, Gasser B, Kinsey K, Oppel S, Scheiblauer S, Couto A, Marra V, Keleman K, Dickson BJ. A genome-wide transgenic RNAi library for conditional gene inactivation in Drosophila. Nature. 2007; 448:151–156. [PubMed: 17625558]

Faas GC, Raghavachari S, Lisman JE, Mody I. Calmodulin as a direct detector of Ca2+ signals. Nature neuroscience. 2011; 14:301–304. [PubMed: 21258328]

Freeman A, Franciscovich A, Bowers M, Sandstrom DJ, Sanyal S. NFAT regulates pre-synaptic development and activity-dependent plasticity in Drosophila. Mol Cell Neurosci. 2011; 46:535–547. [PubMed: 21185939]

Gillespie JM, Hodge JJ. CASK regulates CaMKII autophosphorylation in neuronal growth, calcium signaling, and learning. Front Mol Neurosci. 2013; 6:27. [PubMed: 24062638]

Griffith LC, Verselis LM, Aitken KM, Kyriacou CP, Danho W, Greenspan RJ. Inhibition of calcium/calmodulin-dependent protein kinase in Drosophila disrupts behavioral plasticity. Neuron. 1993; 10:501–509. [PubMed: 8384859]

Guan B, Hartmann B, Kho YH, Gorczyca M, Budnik V. The Drosophila tumor suppressor gene, dlg, is involved in structural plasticity at a glutamatergic synapse. Curr Biol. 1996; 6:695–706. [PubMed: 8793296]

Gumy LF, Katrukha EA, Kapitein LC, Hoogenraad CC. New insights into mRNA trafficking in axons. Dev Neurobiol. 2014; 74:233–244. [PubMed: 23959656]

Haghighi AP, McCabe BD, Fetter RD, Palmer JE, Hom S, Goodman CS. Retrograde control of synaptic transmission by postsynaptic CaMKII at the Drosophila neuromuscular junction. Neuron. 2003; 39:255–267. [PubMed: 12873383]

Hosaka M, Hammer RE, Sudhof TC. A phospho-switch controls the dynamic association of synapsins with synaptic vesicles. Neuron. 1999; 24:377–387. [PubMed: 10571231]

Jin P, Griffith LC, Murphey RK. Presynaptic calcium/calmodulin-dependent protein kinase II regulates habituation of a simple reflex in adult Drosophila. J Neurosci. 1998; 18:8955–8964. [PubMed: 9787001]

Jing Q, Huang S, Guth S, Zarubin T, Motoyama A, Chen J, Di Padova F, Lin SC, Gram H, Han J. Involvement of microRNA in AU-rich element-mediated mRNA instability. Cell. 2005; 120:623–634. [PubMed: 15766526]

Joiner MA, Griffith LC. CaM kinase II and visual input modulate memory formation in the neuronal circuit controlling courtship conditioning. J Neurosci. 1997; 17:9384–9391. [PubMed: 9364084]

Jung H, Yoon BC, Holt CE. Axonal mRNA localization and local protein synthesis in nervous system assembly, maintenance and repair. Nature reviews. 2012; 13:308–324.

Koh YH, Popova E, Thomas U, Griffith LC, Budnik V. Regulation of DLG localization at synapses by CaMKII-dependent phosphorylation. Cell. 1999; 98:353–363. [PubMed: 10458610]

Koon AC, Ashley J, Barria R, DasGupta S, Brain R, Waddell S, Alkema MJ, Budnik V. Autoregulatory and paracrine control of synaptic and behavioral plasticity by octopaminergic signaling. Nature neuroscience. 2011; 14:190–199. [PubMed: 21186359]

Korkut C, Ataman B, Ramachandran P, Ashley J, Barria R, Gherbesi N, Budnik V. Trans-synaptic transmission of vesicular Wnt signals through Evi/Wntless. Cell. 2009; 139:393–404. [PubMed: 19837038]

Korkut C, Li Y, Koles K, Brewer C, Ashley J, Yoshihara M, Budnik V. Regulation of postsynaptic retrograde signaling by presynaptic exosome release. Neuron. 2013; 77:1039–1046. [PubMed: 23522040]

Krol J, Busskamp V, Markiewicz I, Stadler MB, Ribi S, Richter J, Duebel J, Bicker S, Fehling HJ, Schubeler D, Oertner TG, Schratt G, Bibel M, Roska B, Filipowicz W. Characterizing light-regulated retinal microRNAs reveals rapid turnover as a common property of neuronal microRNAs. Cell. 2010; 141:618–631. [PubMed: 20478254]

Kuromi H, Kidokoro Y. Selective replenishment of two vesicle pools depends on the source of Ca2+ at the Drosophila synapse. Neuron. 2002; 35:333–343. [PubMed: 12160750]

Lahey T, Gorczyca M, Jia XX, Budnik V. The Drosophila tumor suppressor gene dlg is required for normal synaptic bouton structure. Neuron. 1994; 13:823–835. [PubMed: 7946331]

Lee YS, Lee JA, Kaang BK. Regulation of mRNA stability by ARE-binding proteins in synaptic plasticity and memory. Neurobiol Learn Mem. 2015; 124:28–33. [PubMed: 26291750]

Morimoto T, Nobechi M, Komatsu A, Miyakawa H, Nose A. Subunit-specific and homeostatic regulation of glutamate receptor localization by CaMKII in Drosophila neuromuscular junctions. Neuroscience. 2010; 165:1284–1292. [PubMed: 19961909]

Motulsky HJ, Brown RE. Detecting outliers when fitting data with nonlinear regression - a new method based on robust nonlinear regression and the false discovery rate. BMC Bioinformatics. 2006; 7:123. [PubMed: 16526949]

Nesler KR, Sand RI, Symmes BA, Pradhan SJ, Boin NG, Laun AE, Barbee SA. The miRNA pathway controls rapid changes in activity-dependent synaptic structure at the Drosophila melanogaster neuromuscular junction. PLoS One. 2013; 8:e68385. [PubMed: 23844193]

Pradhan SJ, Nesler KR, Rosen SF, Kato Y, Nakamura A, Ramaswami M, Barbee SA. The conserved P body component HPat/Pat1 negatively regulates synaptic terminal growth at the larval Drosophila neuromuscular junction. Journal of cell science. 2012; 125:6105–6116. [PubMed: 23097047]

Scott DA, Das U, Tang Y, Roy S. Mechanistic logic underlying the axonal transport of cytosolic proteins. Neuron. 2011; 70:441–454. [PubMed: 21555071]

Shakiryanova D, Morimoto T, Zhou C, Chouhan AK, Sigrist SJ, Nose A, Macleod GT, Deitcher DL, Levitan ES. Differential control of presynaptic CaMKII activation and translocation to active zones. J Neurosci. 2011; 31:9093–9100. [PubMed: 21697360]

Stefani G, Onofri F, Valtorta F, Vaccaro P, Greengard P, Benfenati F. Kinetic analysis of the phosphorylation-dependent interactions of synapsin I with rat brain synaptic vesicles. J Physiol. 1997; 504(Pt 3):501–515. [PubMed: 9401959]

Steward O. mRNA at synapses, synaptic plasticity, and memory consolidation. Neuron. 2002; 36:338–340. [PubMed: 12408837]

Sun XX, Hodge JJ, Zhou Y, Nguyen M, Griffith LC. The eag potassium channel binds and locally activates calcium/calmodulin-dependent protein kinase II. The Journal of biological chemistry. 2004; 279:10206–10214. [PubMed: 14699099]

Sutherland DJ, Pujic Z, Goodhill GJ. Calcium signaling in axon guidance. Trends in neurosciences. 2014; 37:424–432. [PubMed: 24969461]

Takamatsu Y, Kishimoto Y, Ohsako S. Immunohistochemical study of Ca2+/calmodulin-dependent protein kinase II in the Drosophila brain using a specific monoclonal antibody. Brain research. 2003; 974:99–116. [PubMed: 12742628]

Tao-Cheng JH, Dosemeci A, Winters CA, Reese TS. Changes in the distribution of calcium calmodulin-dependent protein kinase II at the presynaptic bouton after depolarization. Brain Cell Biol. 2006; 35:117–124. [PubMed: 17957478]

Thomas M, Lieberman J, Lal A. Desperately seeking microRNA targets. Nat Struct Mol Biol. 2010; 17:1169–1174. [PubMed: 20924405]

Vasin A, Zueva L, Torrez C, Volfson D, Littleton JT, Bykhovskaia M. Synapsin regulates activity-dependent outgrowth of synaptic boutons at the Drosophila neuromuscular junction. J Neurosci. 2014; 34:10554–10563. [PubMed: 25100589]

Wang Z, Palmer G, Griffith LC. Regulation of Drosophila Ca2+/calmodulin-dependent protein kinase II by autophosphorylation analyzed by site-directed mutagenesis. J Neurochem. 1998; 71:378–387. [PubMed: 9648887]

Wang Z, Wilson GF, Griffith LC. Calcium/calmodulin-dependent protein kinase II phosphorylates and regulates the Drosophila eag potassium channel. The Journal of biological chemistry. 2002; 277:24022–24029. [PubMed: 11980904]

Wen Z, Guirland C, Ming GL, Zheng JQ. A CaMKII/calcineurin switch controls the direction of Ca(2+)-dependent growth cone guidance. Neuron. 2004; 43:835–846. [PubMed: 15363394]

## Highlights

- CamKII is enriched in axon terminals at the *Drosophila* neuromuscular junction.
- Presynaptic CamKII is necessary to control activity-dependent synaptic growth.
- Spaced depolarization causes a translation-dependent increase in CamKII levels.
- Phosphorylated CamKII is enriched at the presynaptic membrane in axon terminals.
- CamKII is a target for repression by activity-regulated miR-289.

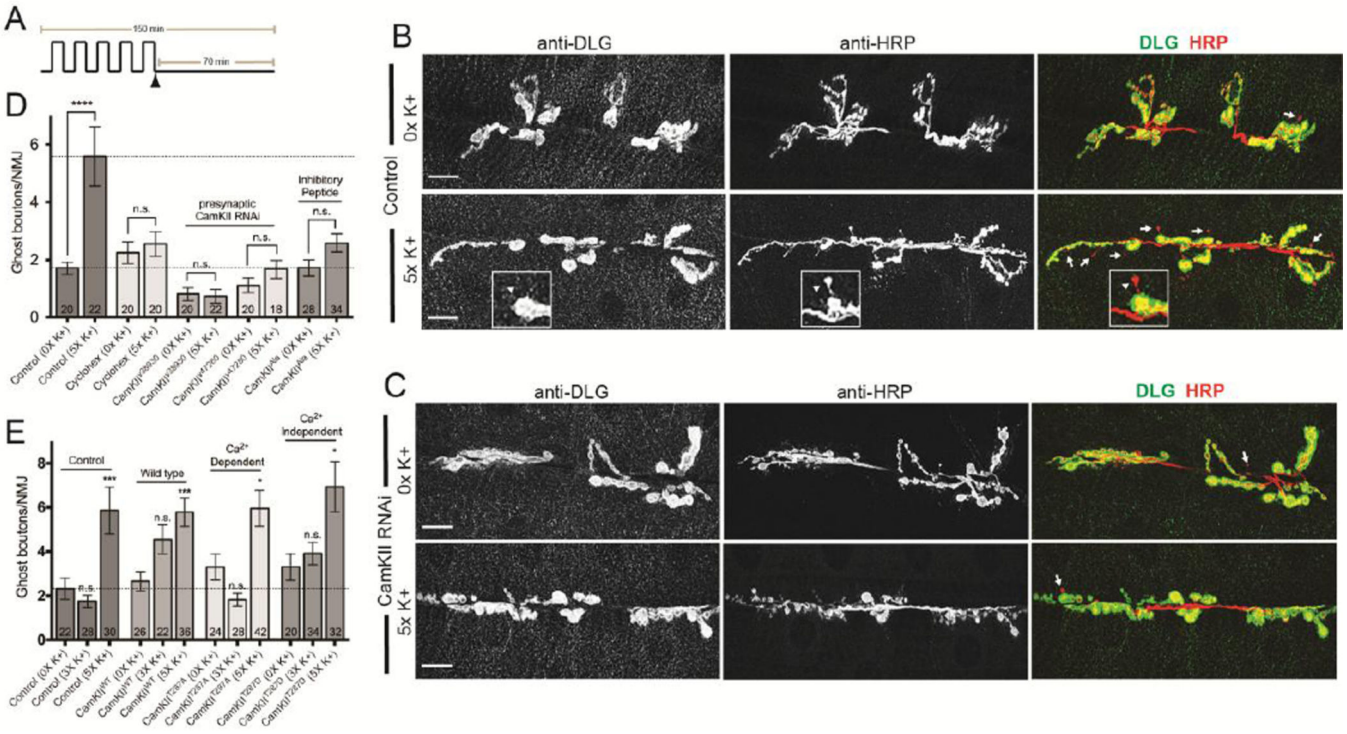


**Figure 1. Presynaptic CamKII is required to control activity-dependent axon terminal growth**

(A) Diagram of the 5X high $K^+$ spaced training paradigm. Partially dissected larval NMJ preps were exposed to a series of five pulses of HL3 containing high $K^+$ (90 mM KCl) separated by rest periods in normal buffer (5 mM KCl). In experiments indicated, cyclohexamide (100 mM) was added to normal HL3 immediately preceding the final ~70 minute rest period (indicated by the arrowhead). (B and C) Larvae were exposed to 0X and 5X high $K^+$ spaced synaptic stimulation and, at the end of the final rest period, preps were fixed and labeled with antibodies against postsynaptic DLG (green) and presynaptic HRP (red). Larger confocal images show an entire synaptic arbor at muscle 6 and 7 in abdominal segment 3. Arrows in (B) and (C) and the arrowhead in (B; inset) point to ghost boutons which are characterized as HRP+ and DLG- presynaptic extensions. Genotypes shown are (B) a *Canton-S* control and (C) a larval prep expressing a transgenic *CamKII* RNAi construct in motor neurons (*C380 > CamKII$^{v38930}$*). (D) The number of ghost boutons following 5X high $K^+$ depolarization in *Canton-S* controls, *Canton-S* controls treated with cyclohexamide, and in different genetic backgrounds to either knock down presynaptic CamKII expression (*C380>CamKII$^{v38930}$* and *C380>CamKII$^{v47280}$*) or disrupt its presynaptic function (*C380>CamKII$^{Ala}$*). (E) The number of ghost boutons following 3X and 5X high $K^+$ depolarization in controls (*C380/+*) and genetic backgrounds that express wild-type (*C380>CamKII$^{WT}$*) or mutant forms (*C380>CamKII$^{T287A}$* or *C380>CamKII$^{T287D}$*) of CamKII in motor neurons. (D and E) The numbers of NMJs analyzed are indicated within each column. * $p < 0.05$, *** $p < 0.001$, **** $p < 0.0001$. The error bars indicate the SEM.

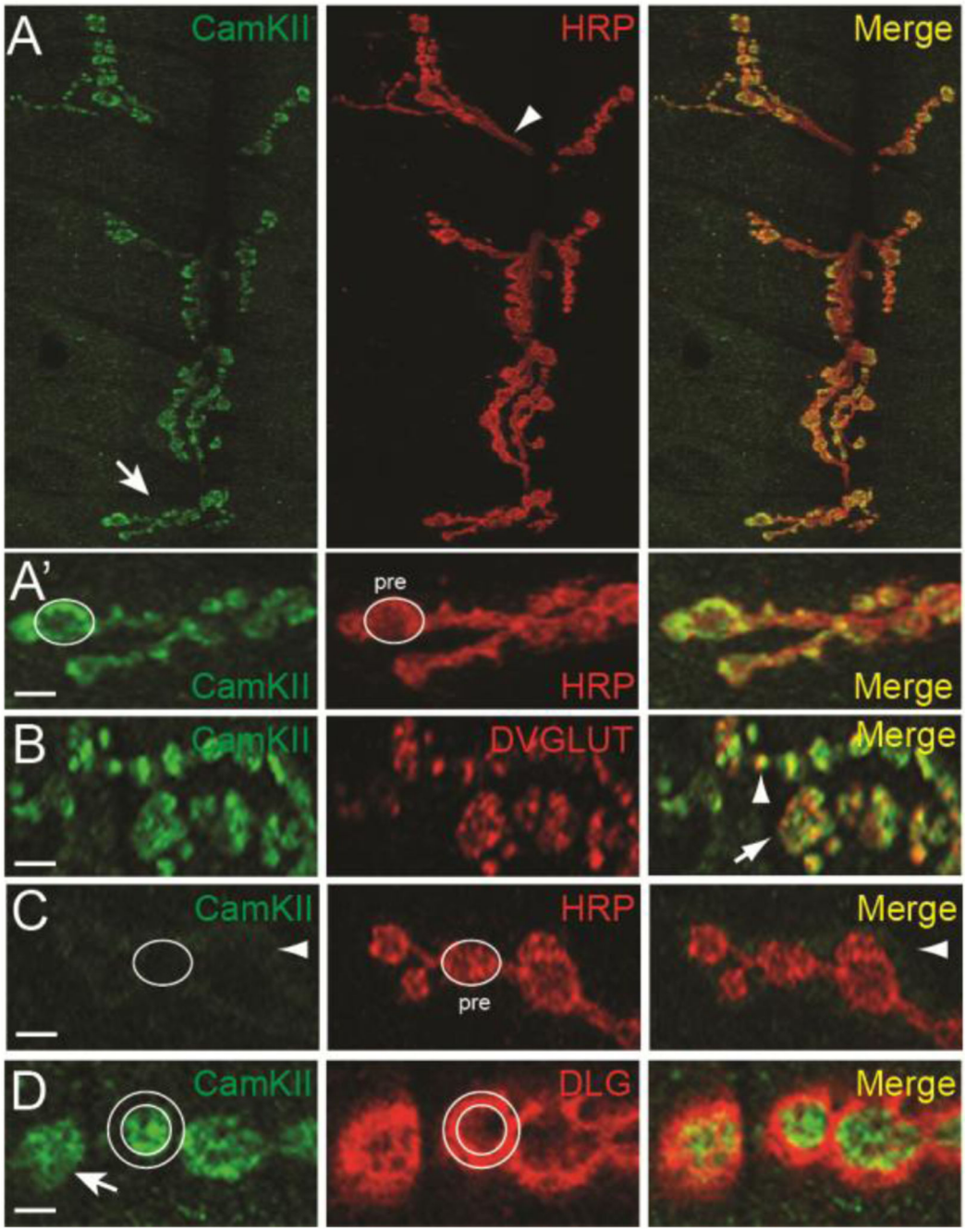


**Figure 2. CamKII is enriched in presynaptic boutons**

(A) CamKII immunoreactivity in the entire synaptic arbor at muscle 6 and 7 in abdominal segment 3. *Canton-S* larvae were double labeled with a monoclonal antibody against CamKII (green) (Takamatsu et al., 2003) and against HRP (red). The arrow in (A) points to type I synaptic boutons shown in (A') while the arrowhead points to the axon innervating the synaptic arbor. In (A') an oval has been drawn around the axon terminal as defined by HRP staining and then superimposed on the green channel. Note that CamKII colocalizes with HRP within the presynaptic bouton. (B) Single confocal section of boutons of NMJs from

larvae stained with monoclonal CamKII (green) and anti-DVGLUT (red) antibodies. The arrow indicates a type 1b synaptic bouton with green, red, and yellow foci. Note that there is a significant amount of overlap (arrowhead) between CamKII and DVGLUT. (C) CamKII immunoreactivity in presynaptic terminals from larvae where CamKII has been knocked down in motor neurons by RNAi (*C380>CamKII*$^{v38930}$). An oval has been drawn around the axon terminal as defined by HRP staining in the red channel and then superimposed onto the monoclonal CamKII (green) channel. Presynaptic CamKII immunostaining has been almost completely eliminated leaving a faint halo of immunoreactivity around the bouton border (arrow). (D) Single confocal section of boutons double stained with a polyclonal antibody against CamKII (green) (Koh et al., 1999) and against DLG (red). Two circles have been drawn to highlight the inner and outer boundaries of DLG staining and then superimposed on the green channel. Note that CamKII staining is largely restricted to the region inside the inner circle indicating enrichment with the axon terminal. Scale bar is 7.5 μm in (A) and 2.5 μm in (A'–D).

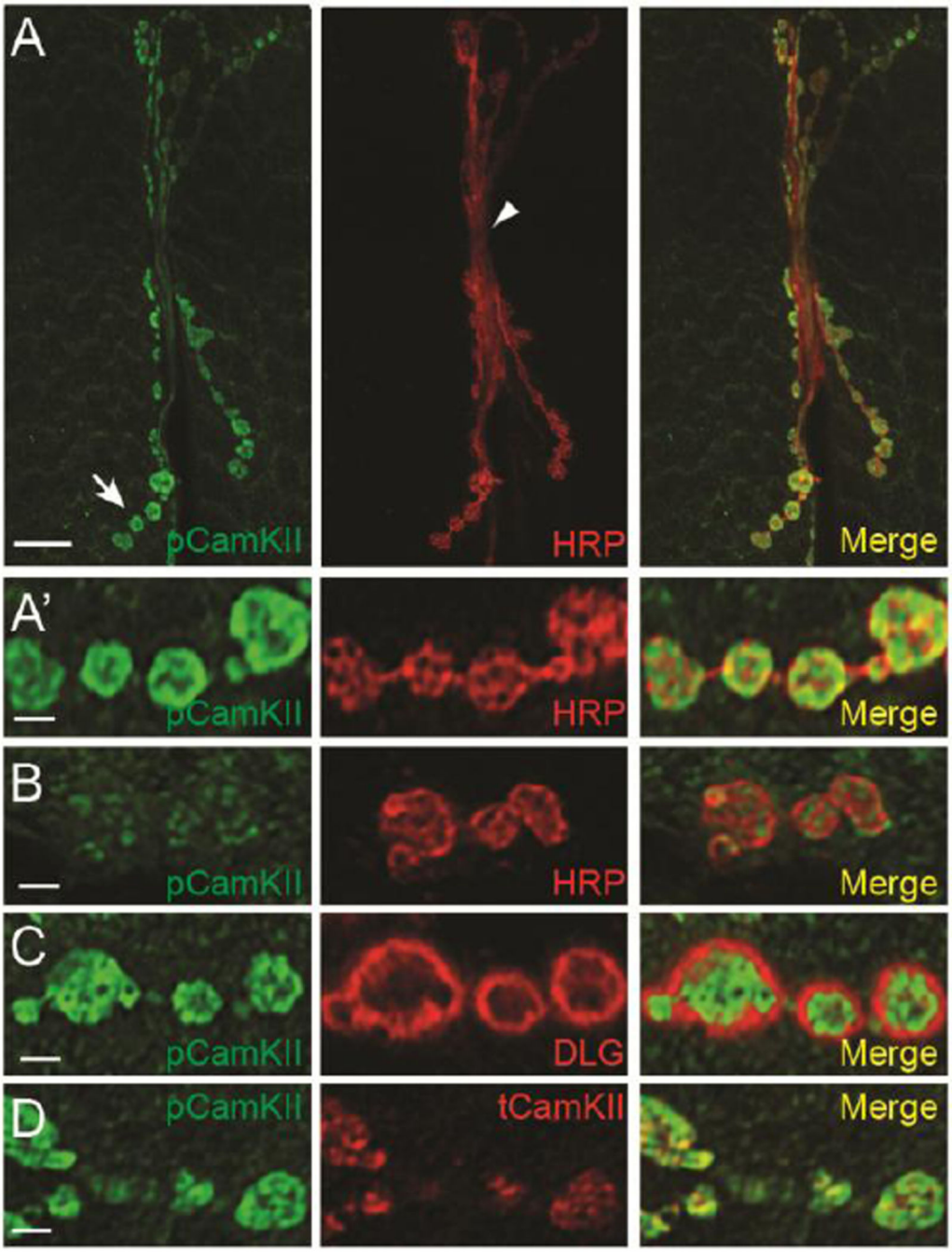


**Figure 3. p-CamKII is enriched in presynaptic boutons**

(A) p-CamKII immunoreactivity in the entire synaptic arbor at muscle 6 and 7 in abdominal segment 3. $w^{1118}$ larvae were double labeled with a monoclonal antibody against p-CamKII (green) (Gillespie and Hodge, 2013) and against HRP (red). The arrow in (A) points to type I synaptic boutons shown in (A') while the arrowhead points to the axon innervating the synaptic arbor. (B) p-CamKII immunoreactivity in presynaptic terminals from larvae where CamKII has been knocked down in motor neurons by RNAi (*C380>CamKII*$^{v38930}$). Presynaptic p-CamKII immunostaining has been almost completely eliminated. (C) Single

confocal section of boutons double stained with an antibody against p-CamKII (green) and against DLG (red). Note that p-CamKII immunoreactivity is restricted to the region inside the circle of DLG staining indicating enrichment with the axon terminal. (D) Single confocal section of boutons of NMJs from larvae stained with p-CamKII (green) and monoclonal anti-CamKII (red) antibodies. Note that there is a significant amount of overlap between p-CamKII and total CamKII. Scale bar is 7.5 μm in (A) and 2.5 μm in (A'–D).

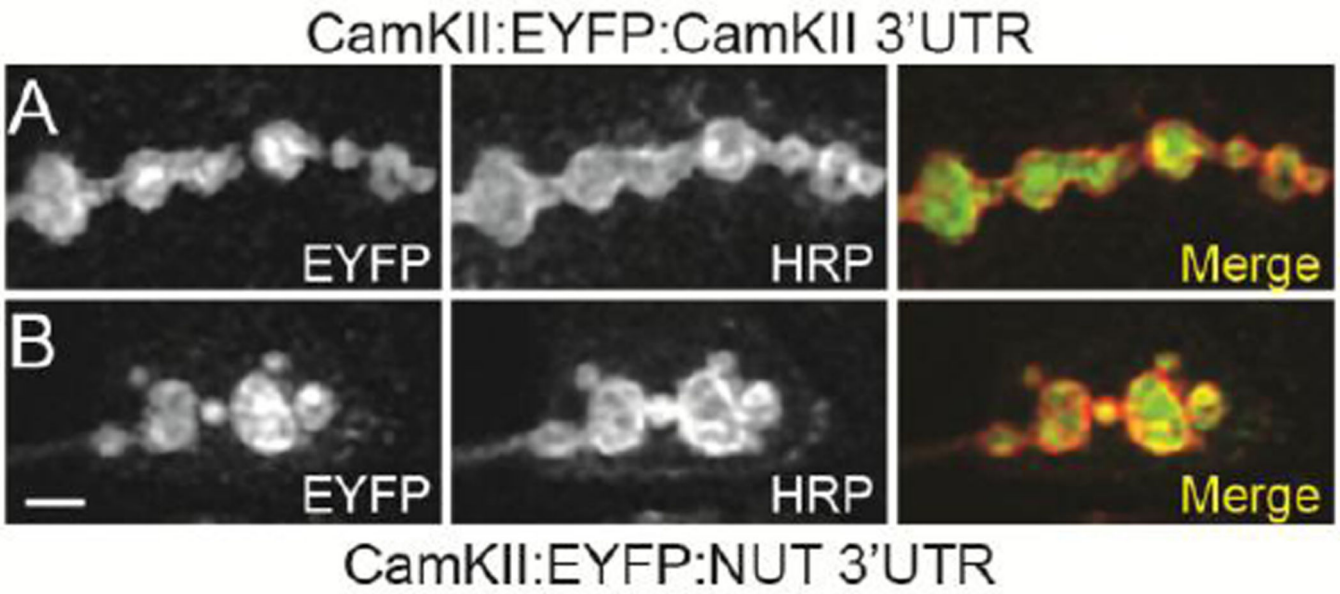


**Figure 4. Enrichment of CamKII in presynaptic boutons does not require the regulatory 3'UTR**

(A–B) Confocal images of NMJs at muscle 6 and 7 in abdominal segment 3 double stained with antibodies against GFP (green) and HRP (red). Larvae shown are expressing a transgene containing a wild-type CamKII protein fused to EYFP controlled by either (A) the *CamKII* regulatory 3'UTR or (B) an unrelated 3'UTR (*C830>UAS-CamKII:EYFP-CamKII 3'UTR* and *C830>UAS-CamKII:EYFP-NUT 3'UTR* respectively). Scale bar is 2.5 μm in (A–B).

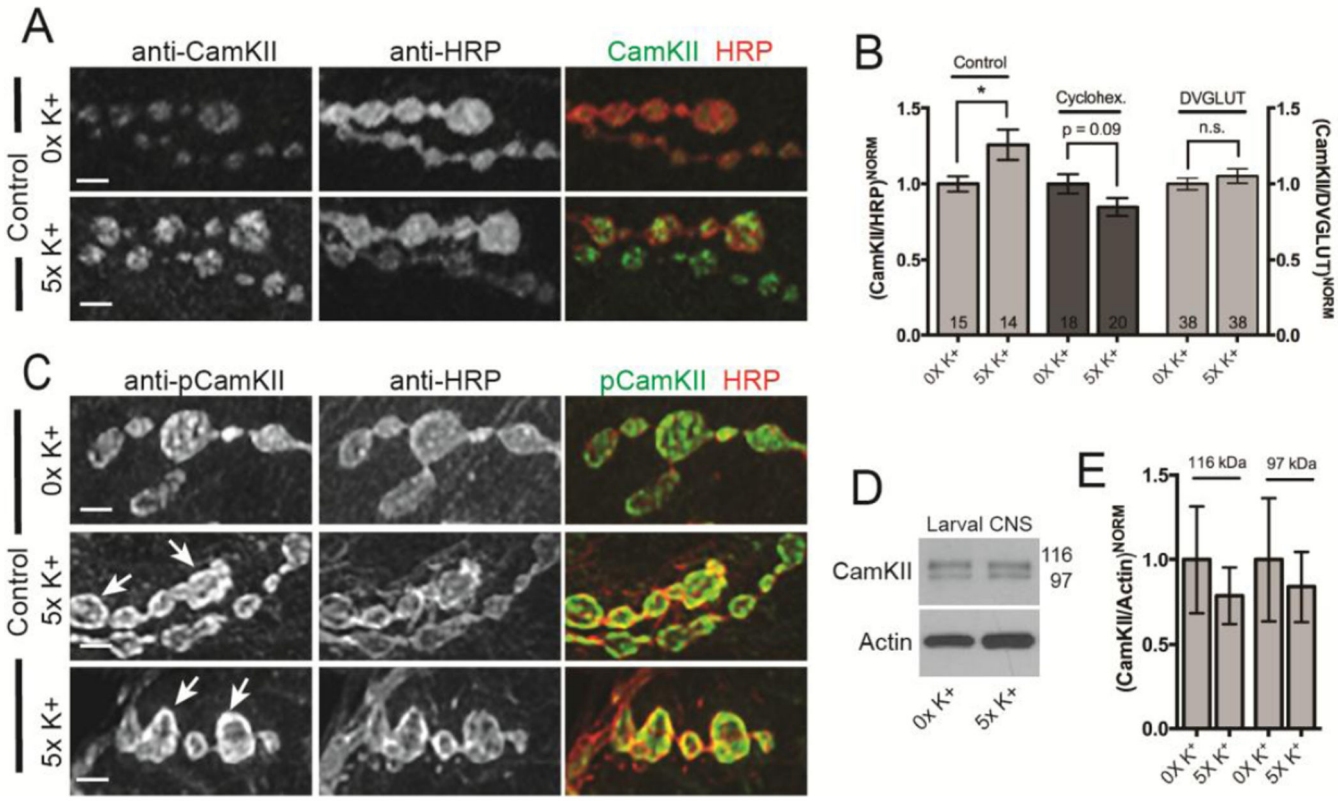


**Figure 5. CamKII enrichment in presynaptic boutons is altered by synaptic activity**

(A, C) Confocal images of NMJs at muscle 6 and 7 in abdominal segment 3. Larvae were exposed to 0X and 5X high $K^+$ spaced synaptic stimulation, fixed, and then double stained with a monoclonal antibody against CamKII or p-CamKII (green) and against HRP (red). Images in both the red and green channels were first thresholded for NMJs from the 5X high $K^+$ stimulation group and the exact same settings used to acquire images from paired controls from the 0X high $K^+$ group. Scale bar is 2.5 μm. (B) Quantification of the immunofluorescence from images from (A) and for NMJs double stained with antibodies against CamKII and DVGLUT. CamKII immunofluorescence in each condition is normalized to either HRP (*Canton-S* control and cyclohexamide-treated *Canton-S* control) or DVGLUT and then 0X high $K^+$ set to 100%. * $p < 0.05$. The numbers of NMJs analyzed are indicated within each column. (D) Representative Western blot of CamKII in larval CNS extracts from *Canton-S* control animals after 0X and 5X high $K^+$ spaced synaptic stimulation. Molecular weights for CamKII isoforms are in kDa. (E) Quantification of the levels of CamKII expression (both bands) normalized to actin from 3 independent biological replicates as shown in (C). The error bars in (B and D) indicate the SEM.

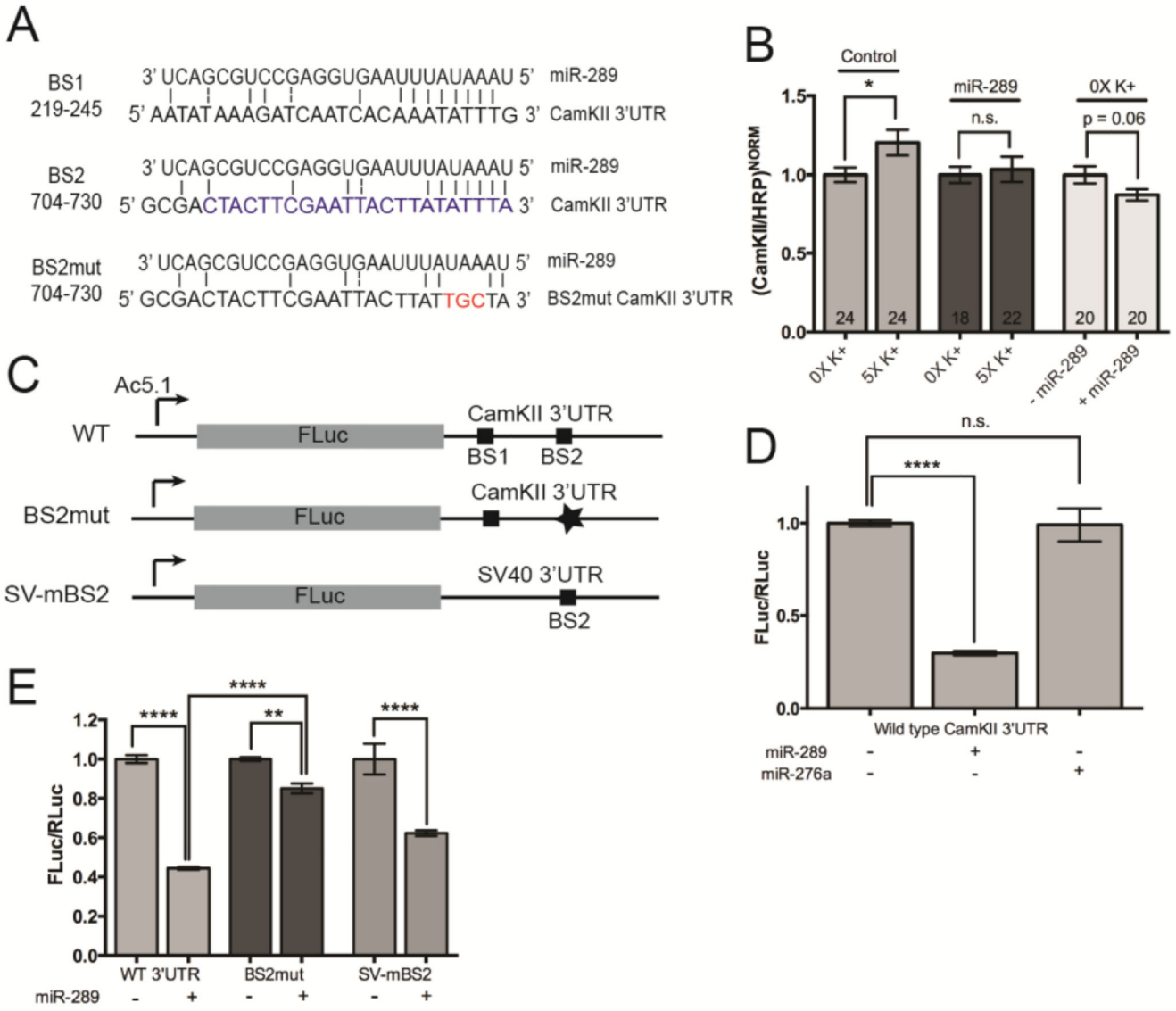


**Figure 6. Expression of CamKII is regulated by miR-289**

(A) Two putative miR-289 binding sites within the *CamKII* 3'UTR. A vertical bar ("|") indicates perfect complementation and a ":" indicates G, U base pairing. The blue sequence in binding site 2 (BS2) indicates the minimal miR-289 binding site. The red sequences indicate the nucleotides at positions 3–6 in the seed region binding site that were mutated in BS2 (BS2mut). (B) Quantification of the immunofluorescence from images from control larvae (*C380/+*) and larvae expressing a transgenic pri-miR289 construct in motor neurons (*C380>UAS-pri-miR289*). NMJs were double stained with antibodies against CamKII and HRP and normalized as described in Fig. 4. Note that miR-289 suppresses the activity dependent increase of CamKII immunofluorescence in axon terminals. Overexpression of miR-289 also reduces overall CamKII levels in unstimulated presynaptic boutons relative to controls (*C380/+*). (C) Diagram of FLuc reporters. The wild-type (WT) reporter as fused to the *CamKII* regulatory 3'UTR. Squares indicate the relative locations of miR-289 BS1 and BS2. The star in BS2mut indicates the mutant BS2 binding site. In SV-mBS2, the minimal

miR-289 binding site in BS2 was introduced into the Simian virus 40 (SV40) 3'UTR and fused downstream of the FLuc coding sequence. (D) *Drosophila* S2 cells were transfected with the FLuc-WT reporter, a RLuc vector, and either an empty vector control or plasmids expressing the indicated miRNAs. Luceferase activity was measured 72 hours after transfection. FLuc values were normalized to RLuc and the empty vector control set to 100%. (E) S2 cells were transfected with FLuc reporters and either an empty vector or plasmid expressing miR-289. Luciferase activity was read and values normalized as described in (D). Error bars in (D–E) indicate the SEM for three biological replicates. ** $p < 0.01$ **** $p < 0.0001$.